Supporting Information

Xia and Springer 10.1073/pnas.1420645111

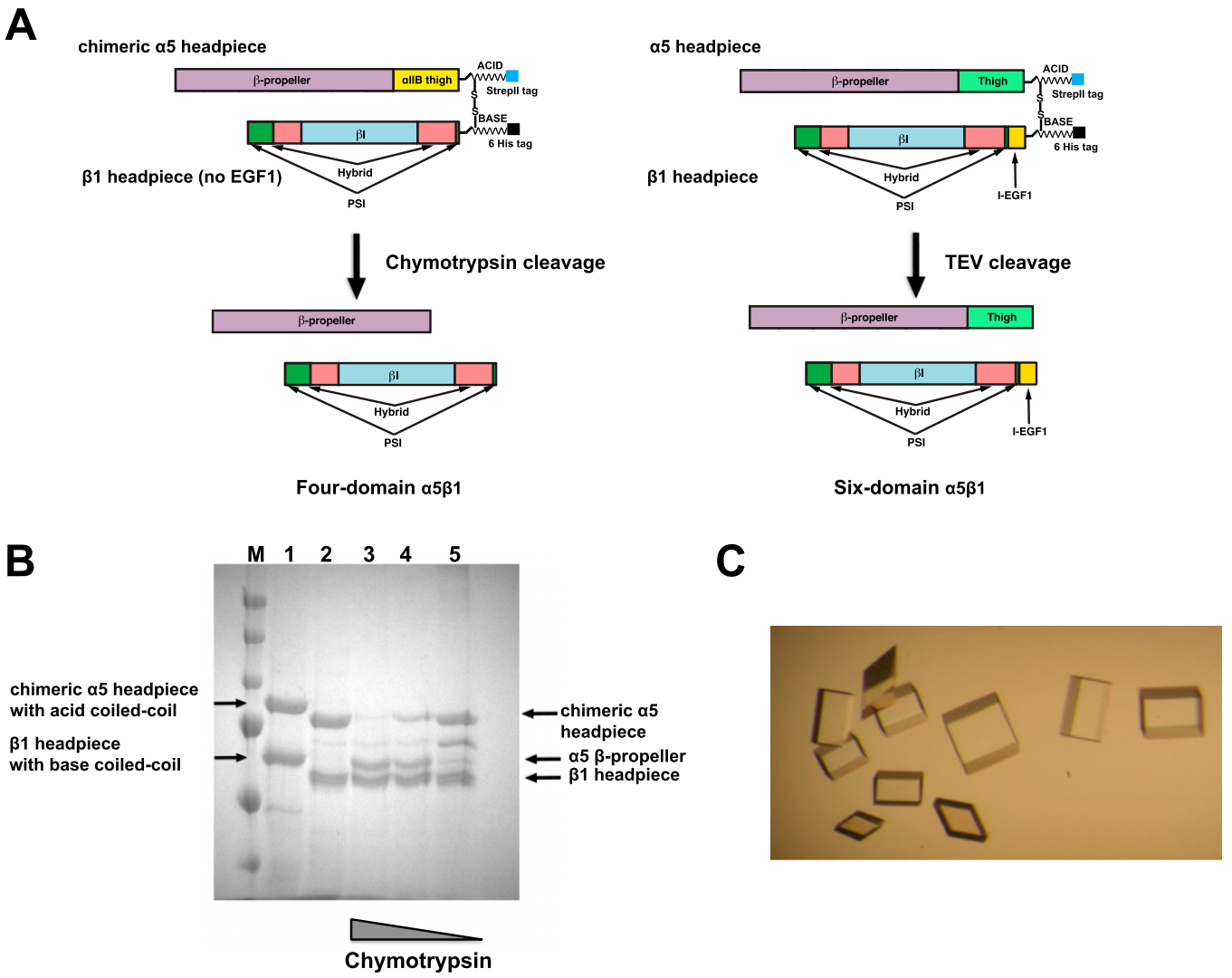

Fig. S1. $\alpha_5\beta_1$ headpiece construct design, protease digestion, and crystallization. (*A*) Schematic illustration of chimeric $\alpha_5\beta_1$ headpiece (*Left*) and wild-type $\alpha_5\beta_1$ headpiece (*Right*) constructs. (*B*) Cleavage of the thigh domain of chimeric protein analyzed by reducing SDS/PAGE. Lanes: M, markers; 1, control uncleaved integrin; 2–5, various protease:integrin ratios (wt:wt); 2, TEV:integrin 1:4; 3, chymotrypsin:integrin 1:100; 4, chymotrypsin:integrin 1:200; 5, chymotrypsin:integrin 1:500. (*C*) Crystals of the four-domain $\alpha_5\beta_1$ headpiece after microseeding.

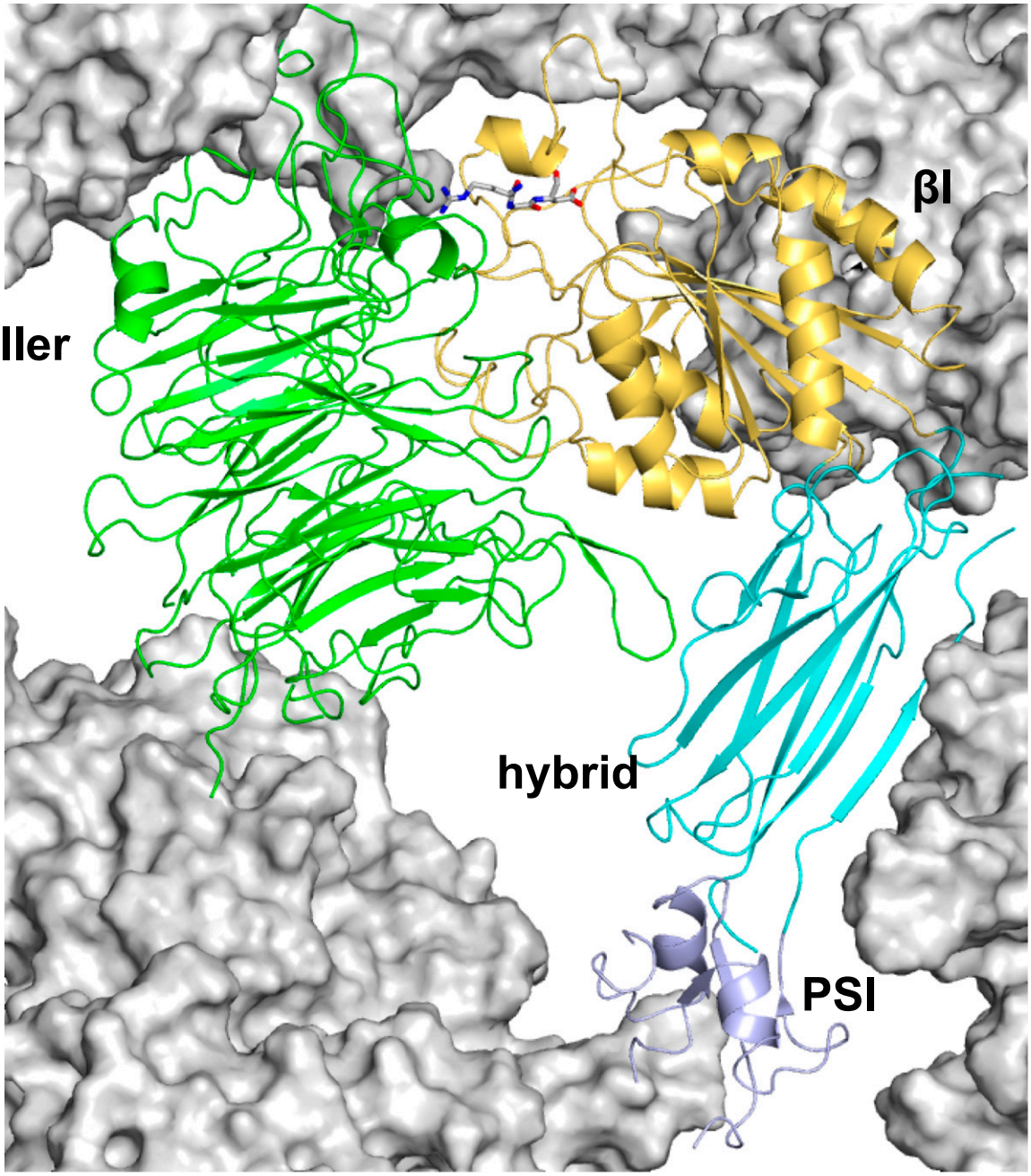

Fig. S2. Crystal lattice contacts of the $\alpha_5\beta_1$ complex with linear RGD in Ca^{2+}/Mg^{2+}. The β-propeller, βI, hybrid, PSI, and RGD are colored green, yellow orange, cyan, light blue, and silver, respectively. Neighboring molecules in the lattice are shown as gray surfaces.

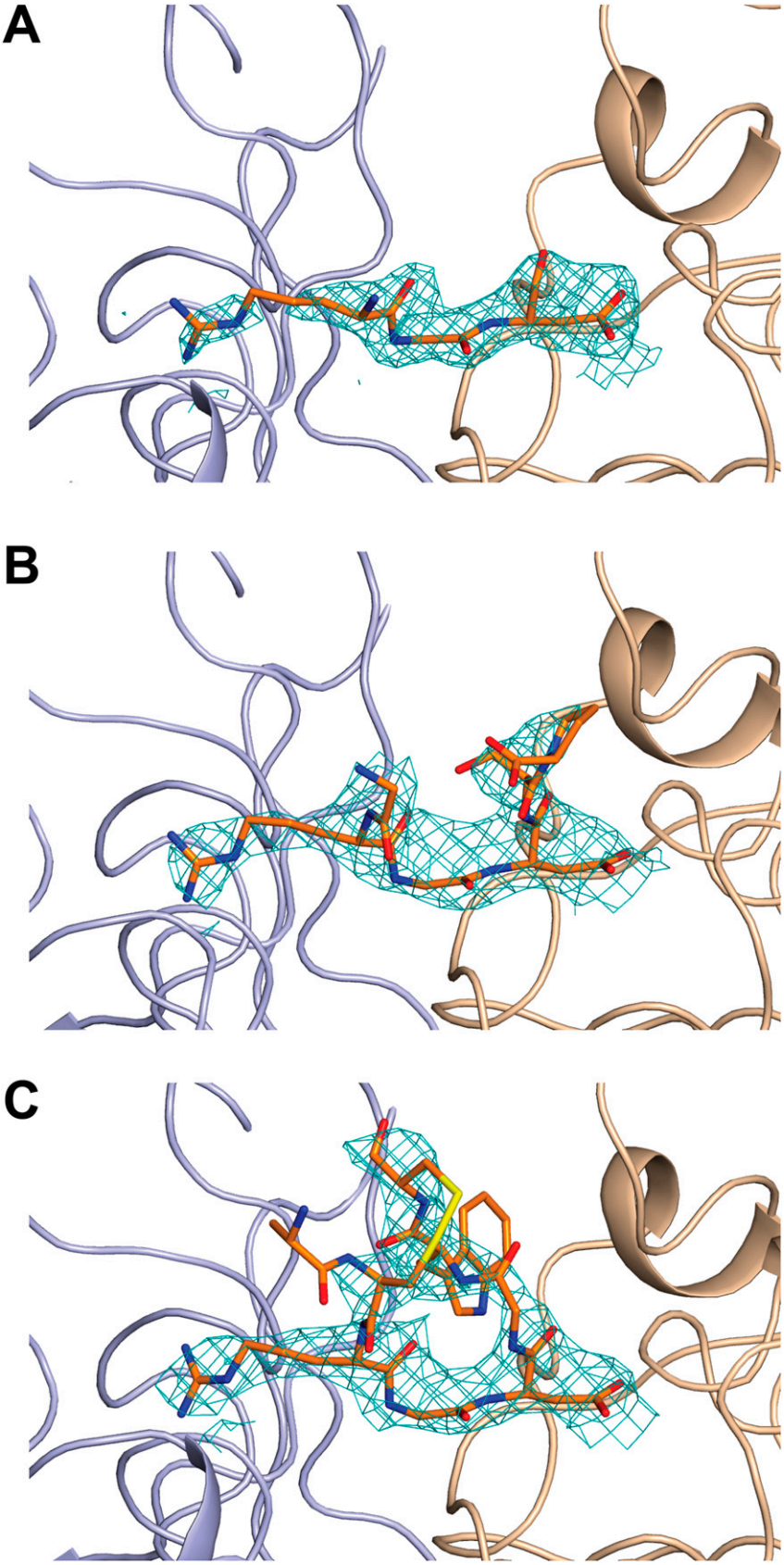

Fig. S3. Density of bound ligands. Simulated-annealing omit maps for GRGDSP peptide soaked in the presence (*A*) and absence (*B*) of Ca^{2+} and for cyclic ACRGDGWCG peptide (*C*). Ligands (orange) are shown in stick representation. The $2F_o - F_c$ simulated-annealing ligand omit map densities (cyan) are shown in mesh at 1σ. α_5 (light blue) and β_1 (wheat) are shown as cartoons.

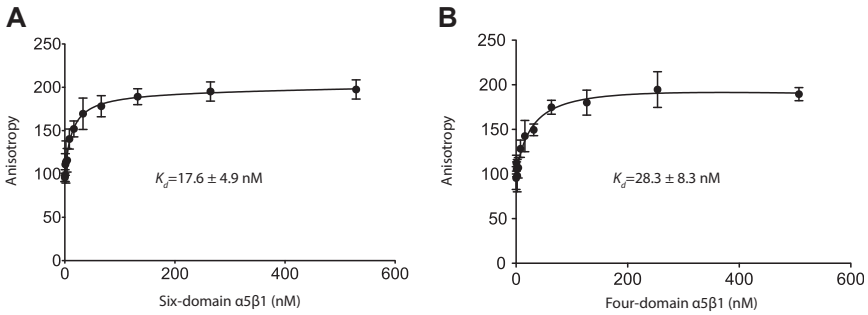

Fig. S4. Fluorescence anisotropy saturation binding. Saturation binding of six-domain $\alpha_5\beta_1$ integrin (*A*) and four-domain $\alpha_5\beta_1$ integrin (*B*) to FITC-aminohexyl-A*CRGDGWC*G cyclic peptide. Experiments were performed in 20 mM Tris-buffered saline with 1 mM Mn^{2+} and 0.1 mM Ca^{2+} (pH 7.4) with 2 nM FITC cyclic RGD peptide. Data represent mean ± SD of triplicate samples.

Table S1. Data collection and refinement statistics

	$\alpha_5\beta_1$	$\alpha_5\beta_1$ + GRGDSP + 5 mM Mg^{2+}/1 mM Ca^{2+}	$\alpha_5\beta_1$ + GRGDSP + 5 mM Mg^{2+}	$\alpha_5\beta_1$ + ACRGDGWCG + 1 mM Mg^{2+}/1 mM Ca^{2+}
Data				
Space group	$P2_12_12_1$	$P2_12_12_1$	$P2_12_12_1$	$P2_12_12_1$
Cell dimensions				
a, *b*, *c*, Å	52.1, 116.8, 159.5	61.1, 117.1, 167.1	61.0, 118.4, 170.3	57.5, 112.2, 169.6
α, β, γ, °	90, 90, 90	90, 90, 90	90, 90, 90	90, 90, 90
Resolution, Å	47.1–1.85	47.94–1.78	42.57–2.50	47.60–2.50
Reflections, total/unique	292,419/82,697	410,297/113,328	157,294/42,741	140,454/38,535
Completeness, %	98.4 (93.5)	98.2 (99.6)	98.2 (99.7)	99.3 (99.9)
$CC_{1/2}$, %[†]	99.4 (16.9)	99.4 (11.8)	99.6 (28.2)	99.6 (19.2)
*CC**, %[‡]	99.9 (53.7)	99.8 (45.9)	99.9 (60.4)	99.9 (56.8)
I/σ(I)	6.55 (0.45)	7.17 (0.34)	7.46 (0.62)	7.17 (0.66)
R_{merge}, %[§]	12.6 (210.7)	15.4 (342.2)	14.4 (276.3)	10.6 (210.0)
Redundancy	3.5 (2.7)	3.6 (3.3)	3.7 (3.7)	3.6 (3.7)
Refinement				
R_{work}	0.191 (0.397)	0.187 (0.423)	0.210 (0.403)	0.187 (0.392)
R_{free}[¶]	0.238 (0.392)	0.223 (0.468)	0.254 (0.455)	0.236 (0.388)
CC_{work}, %[#]	95.9 (39.7)	97.3 (28.8)	94.5 (53.9)	96.5 (46.8)
CC_{free}, %[#]	94.6 (36.5)	94.9 (39.8)	93.3 (48.4)	94.6 (37.8)
Ramachandran, %[‖]	96.0/3.7/0.3	96.2/3.7/0.1	95.5/4.3/0.2	93.7/5.9/0.4
Bond rmsd, Å	0.011	0.007	0.003	0.005
Angle rmsd, °	1.06	1.09	0.71	0.98
MolProbity score**	1.15 (99%)	1.24 (99%)	1.26 (100%)	1.40 (100%)
Clash score	1.38 (100%)	2.12 (99%)	1.88 (100%)	2.12 (100%)
PDB ID code	4WJK	4WK0	4WK2	4WK4

Values for highest-resolution shells are in parentheses.

[†]$CC_{1/2}$ = Pearson's correlation coefficient between average intensities of random half-datasets for each unique reflection.

[‡]$CC^* = \sqrt{2CC1/2/(1+CC1/2)}$.

[§]$R_{merge} = \sum i,h|I(i,h) - \langle I(h)\rangle|/\sum i,h|I(i,h)|$, where $I(i,h)$ and $\langle I(h)\rangle$ are the *i*th and mean measurement of intensity of reflection *h*.

[¶]R_{free} was calculated using 5% of the data.

[#]Correlation coefficients of the observed intensities with the model-based intensities for the work (CC_{work}) and test (CC_{free}) sets.

[‖]Residues in favored, accepted, and outlier regions of the Ramachandran plot as reported by MolProbity.

**MolProbity (1) score and percentile among structures of comparable resolution.

1. Chen VB, et al. (2010) MolProbity: All-atom structure validation for macromolecular crystallography. *Acta Crystallographica* D66:12–21.

Table S2. Real space cross-correlation as a measure of occupation of metal and ligand binding sites

		βI domain metal binding sites			β-Propeller domain β-hairpin Ca^{2+} sites				RGD		
Structure	Å	SyMBS	MIDAS	ADMIDAS	Hairpin 1	Hairpin 2	Hairpin 3	Hairpin 4	Arg	Gly	Asp
$\alpha_5\beta_1$	1.85	0.92/0.91	0.91/0.95	0.93/0.94	0.94/0.94	0.92/0.90	0.90/0.88	0.90/0.89	—	—	—
$\alpha_5\beta_1$ + RGD + Ca^{2+}	1.78	0.93/0.89	0.90/0.95	0.92/0.95	0.92/0.94	0.93/0.95	0.94/0.90	0.93/0.93	0.79/0.82	0.86/0.87	0.85/0.87
$\alpha_5\beta_1$ + RGD − Ca^{2+}	2.50	0.78/0.80	0.83/0.80	0.46/0.53	0.92/0.90	0.83/0.79	0.80/0.81	0.72/0.77	0.79/0.80	0.82/0.87	0.84/0.88
$\alpha_5\beta_1$ + cyclic RGD + Ca^{2+}	2.50	0.91/0.92	0.86/0.93	0.61/0.65	0.87/0.90	0.85/0.87	0.77/0.79	0.74/0.78	0.83/0.90	0.89/0.91	0.89/0.89
Nagae et al. (1) $\alpha_5\beta_1$ mol. 1	2.90	0.76/0.79	0.55/0.88	0.64/0.86	0.92/0.91	0.72/0.89	0.37/0.91	0.770.76	—	—	—
Nagae et al. $\alpha_5\beta_1$ mol. 1	2.90	0.53/0.93	0.57/0.84	0.72/0.89	0.67/0.89	0.61/0.83	0.50/0.91	0.65/0.89	—	—	—
Nagae et al. $\alpha_5\beta_1$ + RGD mol. 1	2.90	0.81/0.87	0.68/0.87	0.52/0.36	0.68/0.90	0.77/0.83	0.30/0.93	0.72/0.66	0.30/0.67	0.50/0.82	0.64/0.82
Nagae et al. $\alpha_5\beta_1$ + RGD mol. 2	2.90	0.61/0.91	0.75/0.90	0.73/0.68	0.64/0.89	0.56/0.86	0.65/0.92	0.67/0.81	0.56/0.71	0.59/0.77	0.70/0.84

As an estimate of occupation and order of bound metal ions and ligand, the real space cross-correlation between electron density and the molecular model was calculated. RSCC values (value 1/value 2) are shown with two types of maps, simulated-annealing composite omit map density (value 1) and simulated-annealing maps with ligand and all metals omitted (value 2). For RSCC calculation, Ca^{2+} was added to the ADMIDAS of the RGD-bound (1) structure. mol., molecule.

1. Nagae M, et al. (2012) Crystal structure of α5β1 integrin ectodomain: Atomic details of the fibronectin receptor. *J Cell Biol* 197(1):131–140.

Table S3. Variation in β-hybrid and β-PSI interdomain angle

Structures	Angles
$\alpha_5\beta_1/\alpha_5\beta_1$ with linear RGD[†]	8.5°
$\alpha_5\beta_1/\alpha_5\beta_1$ with linear RGD soaked without Ca^{2+}[†]	10.4°
$\alpha_5\beta1/\alpha_5\beta_1$ with cyclic RGD[†]	9.0°
$\alpha_5\beta_1$/Nagae et al. (1) $\alpha_5\beta_1$ (PDB ID code 3VI3)[‡]	10.3°–12.7°
$\alpha_5\beta_1$/Nagae et al. $\alpha_5\beta_1$ with linear RGD (PDB ID code 3VI4)[‡]	9.8°–14.6°

Two molecules were superimposed using the β-hybrid domain, and the change in angle upon superimposing on the β-PSI domain was calculated.
[†]One molecule in current structures.
[‡]Two molecules in PDB ID codes 3VI3 and 3VI4.

1. Nagae M, et al. (2012) Crystal structure of α5β1 integrin ectodomain: Atomic details of the fibronectin receptor. *J Cell Biol* 197(1):131–140.

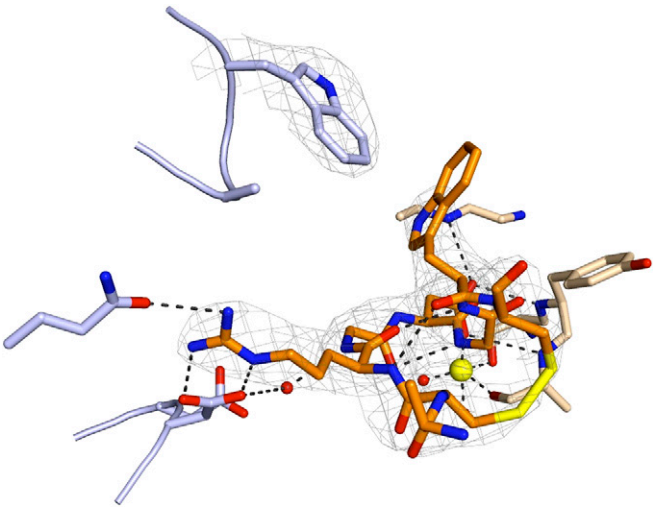

Movie S1. ■■■

Movie S1